Comparative Medicine
Copyright 2010
by the American Association for Laboratory Animal Science

Vol 60, No 4
August 2010
Pages 300–315

Metabolic Syndrome and Coronary Artery Disease in Ossabaw Compared with Yucatan Swine

Zachary P Neeb, Jason M Edwards, Mouhamad Alloosh, Xin Long, Eric A Mokelke, and Michael Sturek*

Metabolic syndrome (MetS), a compilation of associated risk factors, increases the risk of type 2 diabetes and coronary artery disease (CAD, atherosclerosis), which can progress to the point of artery occlusion. Stents are the primary interventional treatment for occlusive CAD, and patients with MetS and hyperinsulinemia have increased restenosis. Because of its thrifty genotype, the Ossabaw pig is a model of MetS. We tested the hypothesis that, when fed high-fat diet, Ossabaw swine develop more features of MetS, greater native CAD, and greater stent-induced CAD than do Yucatan swine. Animals of each breed were divided randomly into 2 groups and fed 2 different calorie-matched diets for 40 wk: control diet (C) and high-fat, high-cholesterol atherogenic diet (H). A bare metal stent was placed in the circumflex artery, and pigs were allowed to recover for 3 wk. Characteristics of MetS, macrovascular and microvascular CAD, in-stent stenosis, and Ca^{2+} signaling in coronary smooth muscle cells were evaluated. MetS characteristics including, obesity, glucose intolerance, hyperinsulinemia, and elevated arterial pressure were elevated in Ossabaw swine compared to Yucatan swine. Ossabaw swine with MetS had more extensive and diffuse native CAD and in-stent stenosis and impaired coronary blood flow regulation compared with Yucatan. In-stent atherosclerotic lesions in Ossabaw coronary arteries were less fibrous and more cellular. Coronary smooth muscle cells from Ossabaw had impaired Ca^{2+} efflux and intracellular sequestration versus cells from Yucatan swine. Therefore, Ossabaw swine are a superior model of MetS, subsequent CAD, and cellular Ca^{2+} signaling defects, whereas Yucatan swine are leaner and relatively resistant to MetS and CAD.

Abbreviations: CAD, coronary artery disease; CSM, coronary smooth muscle; IVGTT, intravenous glucose tolerance test; MetS, metabolic syndrome; SERCA, sarco–endoplasmic reticulum Ca^{2+} ATPase; ET1, endothelin 1; SOCE, store-operated Ca^{2+} entry.

Atherosclerotic coronary artery disease (CAD) is increased at least 2-fold in patients with metabolic syndrome (MetS)[27] and is accompanied by marked microvascular dysfunction that further impairs coronary blood flow.[10] MetS generally is diagnosed by the presence of 3 or more of the following conditions: obesity, insulin resistance, glucose intolerance, dyslipidemia, and hypertension.[17,28] There is strong support for the role of the hyperinsulinemia component of MetS in increased restenosis after percutaneous coronary interventions.[74,75,84,85] Further, our group has shown that severe coronary microvascular dysfunction occurs in MetS.[5] Because MetS (so-called 'prediabetes') affects as much as 27% of the United States population, is increasing dramatically in prevalence,[94] and can progress to type 2 diabetes, there is great need for basic research using animal models that accurately mimic MetS and the accompanying CAD. Clearly, there is need for study of MetS-induced CAD and in-stent stenosis and the underlying cellular and molecular mechanisms.

Mice, rats, and swine are known to recapitulate MetS;[3,12,36,60,71,72] however, none of these models fully reproduce the combined symptoms of MetS and CAD. Further, transgenic mouse models are simply not adequate for coronary vascular interventions using stents identical to those used in humans,[18,23,38,55,57,79,83,86] a step that is essential for translation to the clinic. Yucatan and domestic swine are commonly used large animal models for study of cardiovascular disease due to their ability to mimic the neointimal formation and thrombosis observed in humans.[86] For example, several laboratories have produced severe CAD in swine,[8,24,51,61,62,68,91] but through toxin-induced pancreatic β-cell ablation and feeding of an atherogenic diet, rather than as a natural development subsequent to MetS or diabetes. Currently, there is a paucity of large animal models that reproduce MetS and CAD.[3]

Research on the obesity-prone Ossabaw miniature swine[59] clearly indicates that these animals develop MetS and cardiovascular disease when fed a high-calorie atherogenic diet,[4,5,9,16,19,42,50,52,83,92] Female Ossabaw swine on this type of diet nearly doubled their percentage body fat in only 9 wk, showed insulin resistance, impaired glucose tolerance, dyslipidemia (profound increase in the ratio of low-density to high-density lipoprotein cholesterol, hypertriglyceridemia), hypertension, and early coronary atherosclerosis.[16] These data contrast with those from male Yucatan miniature pigs, which did not develop MetS even after 20 wk on a comparable excess calorie atherogenic diet.[8,68,95] Yucatan swine do not develop MetS through diet manipulation, unlike Ossabaw swine, which consistently recapitulate all MetS characteristics. However, important differences in study design have not allowed direct comparison between Yucatan and Ossabaw swine.

Cytosolic Ca^{2+} signaling is involved in 'phenotypic modulation' of coronary smooth muscle (CSM), as characterized by proliferation and migration in several in vitro cell culture models[33,35,89,90] and in vivo rodent models of the peripheral circulation (for example, reference 51). The Yucatan swine model of diabetic dyslipidemia shows altered Ca^{2+} extrusion,[96] Ca^{2+} sequestration by

Received: 03 Dec 2009. Revision requested: 03 Jan 2010. Accepted: 20 Apr 2010.
Department of Cellular and Integrative Physiology, Indiana University School of Medicine, Indianapolis, Indiana.
Corresponding author. Email: msturek@iupui.edu

the sarcoplasmic reticulum,[32,34,98] and Ca^{2+} influx through voltage-gated Ca^{2+} channels.[98] Currently, Ca^{2+} signaling has not been compared directly between MetS Ossabaw and Yucatan swine CSM. Therefore, the purpose of the present study was to test the hypothesis that compared with Yucatan swine on calorie-matched standard chow (for example, Yucatan maintenance diet[8,95]) and atherogenic diets, Ossabaw swine have a greater propensity to MetS and CAD with impaired coronary microvascular dysfunction and Ca^{2+} handling in CSM.

Materials and Methods

Animal care and use. All protocols involving animals were approved by an institutional animal care and use committee and complied fully with recommendations outlined by the National Research Council and American Veterinary Medical Association.[2,37] Male Ossabaw and Yucatan swine each were assigned to 1 of 4 groups (n = 9 per group): Ossabaw control, Yucatan control, and Ossabaw and Yucatan on high-fat, high-cholesterol, atherogenic diet. The control groups for both breeds were fed a calorie-matched diet for 43 wk, which contained 22% of calories from protein, 70% of calories from carbohydrates, and 8% of calories from fat. The pigs in the control groups received 3200 kcal daily until euthanasia, which was a standard amount for maintaining lean, normal body growth in Yucatan swine.[83] The atherogenic diet was composed of control chow supplemented with (percentage by weight): cholesterol, 2.0%; coconut oil, 17%; corn oil, 2.5%, and sodium cholate, 0.7%. This mixture yielded 13% of calories from protein, 40% of calories from carbohydrates, and 47% of calories from fat. The animals in the atherogenic groups ate 3200 kcal daily (calorie-matched to the control diet) for 43 wk until they were euthanized. The very-high-fat diet was similar to the high-fat diet in matching of calories and duration of feeding, except that the very-high-fat mixture yielded 6% of calories from protein, 19% of calories from carbohydrates, and 75% of calories from fat (n = 8). All animals were housed and fed in individual pens and provided a 12:12-h light:dark cycle. Water was provided ad libitum.

Body composition. Backfat was measured by using ultrasonography and carcass fat was assessed by proximate chemical composition analysis, as previously described.[95] Backfat measurements were taken 1 wk before euthanasia; carcass fat was measured afterward. Body mass index was determined as in humans,[26] as body weight in kg divided by the square of the pig's length from the end of the snout to the base of the tail.

Intravenous glucose tolerance test (IVGTT). Swine were acclimated to restraint in a specialized sling for 5 to 7 d before IVGTT was conducted within 1 wk before stent placement. Swine then were fasted overnight and anesthetized with isoflurane (maintained at 2% by mask with supplemental O_2). The right jugular vein was catheterized percutaneously.[11,16,83] After catheterization, swine were allowed to recover for 3 h before the IVGTT to avoid any effect of isoflurane on insulin signaling.[68] Once recovered from anesthesia, swine were restrained in the sling, and tail cuff blood pressure measurements and baseline blood samples were obtained, as previously described.[68,95] Glucose (0.5 g/kg IV) was administered, and timed blood samples were collected.[68] Blood glucose was measured automatically (YSI 2300 STAT Plus Glucose analyzer, YSI Life Sciences, Yellow Springs, OH). Plasma insulin assays were performed by a commercial laboratory (Linco Research Laboratories, St Charles, MO). Homeostasis model assessment is used to diagnose insulin resistance under fasting conditions.[88] We measured insulin×glucose concentration near their peaks (10 min after bolus glucose injection) during the IVGTT to obtain a modified value for homeostasis model assessment.[16,52]

Plasma lipid assays. Venous blood samples were obtained during the week preceding stent placement after overnight fasting and were analyzed for triglyceride and total cholesterol (fractionated into HDL and LDL components) concentrations. Cholesterol in lipoprotein fractions was determined after precipitation of HDL by using minor modifications of standard methods.[16,93] Specifically, apolipoprotein-B–containing lipoproteins were precipitated with heparin–$MnCl_2$, and the supernatant was assayed. LDL content was calculated from the Friedewald equation:[22]

$$\text{LDL} = \text{total cholesterol} - \text{HDL} - (\text{triglyceride} \div 5).$$

Stent procedure. After 40 wk on the diets, all pigs underwent placement of a bare metal stent in the circumflex coronary artery of all pigs followed by euthanasia 3 wk later, similar to previous reports.[18,19,55,83] Swine received 325 mg aspirin as antiplatelet therapy starting the day prior to the stent procedure and continuing for the 3 wk after stent deployment. After an overnight fast, swine received 0.05 mg/kg atropine, 2.2 mg/kg xylazine, and 5.5 mg/kg Telazol (Fort Dodge Animal Health, Fort Dodge, IA) IM. Swine were intubated, and anesthesia was maintained with 2% to 4% isoflurane in 100% O_2 as a carrier gas. The isoflurane level was adjusted to maintain anesthesia with stable hemodynamics. Heart rate, aortic blood pressure, respiratory rate, and electrocardiographic data were continuously monitored throughout the procedure. Under sterile conditions, a 7-French vascular introducer sheath was inserted into the right femoral artery and heparin (200 U/kg) administered. A 7-French guiding catheter (sizes 0.75 to 2.0; Amplatz L, Cordis, Bridgewater, NJ) was advanced to engage the left main coronary ostium. A 3.2-French, 30-MHz intravascular ultrasound catheter (Boston Scientific, Natick, MA) was advanced over a guide wire and positioned in the coronary artery. A mechanized device pulled the intravascular ultrasound transducer, located within the lumen of the intravascular ultrasound catheter, at a constant rate of 0.5 mm/sec back towards the left main coronary ostium, allowing visualization of the entire length of the coronary artery (a technique termed 'intravascular ultrasound pullback'). Importantly, the intravascular ultrasound catheter remained stationary during the pullback procedure, and the transducer moved within the catheter, thus limiting any mechanical stress on the coronary artery wall. Video images were analyzed offline (Sonos Intravascular Imaging System; Hewlett Packard, Palo Alto, CA).

The intravascular ultrasound catheter was removed, and a coronary stent (diameter, 2.5 to 4.0 mm; length, 8 mm; Express2, Boston Scientific) catheter was deployed. Stents were chosen to match artery diameter at optimal inflation pressure. One stent (diameter, 1.0 × lumen diameter) was placed in the circumflex artery. After stent placement, angiography was repeated followed by reintroduction of the intravascular ultrasound catheter, to confirm correct stent deployment. The intravascular ultrasound catheter, guide catheter, and introducer sheath were removed and the right femoral artery ligated. The incision was closed, and the pig was allowed to recover. Cephalexin (1000 mg) was given twice daily for 6 d after the stent procedure.

Coronary blood flow. The ostium of the left main artery was engaged with the guiding catheter, and a Doppler flow wire (di-

Table 1. Phenotypic characteristics of Yucatan (Y) and Ossabaw (O) swine fed control (C) or high-fat, high-cholesterol atherogenic (H) diet

	Yucatan C	Yucatan H	Ossabaw C	Ossabaw H	$P < 0.05$
Starting body weight (kg)	41.3 ± 9.8	37.3 ± 1.6	43 ± 0.8	44.4 ± 0.7	None
End body weight (kg)	59 ± 2	58 ± 3	74 ± 2	76 ± 2	Y < O
Starting body mass index (kg/m^2)	32 ± 1	34 ± 1	28 ± 1	28 ± 1	Y > O
End body mass index (kg/m^2)	38 ± 1	38 ± 3	47 ± 6	45 ± 1	Y < O
Total cholesterol (mg/dL)	52 ± 4	420 ± 72	62 ± 3	338 ± 28	C < H
HDL (mg/dL)	30 ± 3	60 ± 10	34 ± 1	75 ± 9	C < H
LDL (mg/dL)	14 ± 3	351 ± 76	20 ± 4	255 ± 29	C < H
LDL:HDL	0.5 ± 0.1	6.5 ± 1.6	0.7 ± 0.1	3.9 ± 0.8	C < H
Triglycerides (mg/dL)	38 ± 6	41 ± 6	19 ± 3	41 ± 7	None
Systolic blood pressure (mm Hg)	77 ± 4	79 ± 9	88 ± 7	91 ± 3	None
Diastolic blood pressure (mm Hg)	48 ± 3	54 ± 1	59 ± 8	56 ± 3	None
Mean arterial pressure (mm Hg)	57 ± 4	62 ± 1	68 ± 7	67 ± 3	Y < O
Heart weight/ body weight	0.0039 ± 0.00012	0.00436 ± 0.00023	0.0031 ± 0.0001	0.003 ± 0.00006	Y > O
Coronary artery diameter (mm)	2.7 ± 0.1	2.5 ± 0.1	2.3 ± 0.3	2.3 ± 0.1	Y > O

Two-way ANOVA was performed on each data set. Any significant differences ($P < 0.5$) were reported between groups of swine or diets (within each breed).

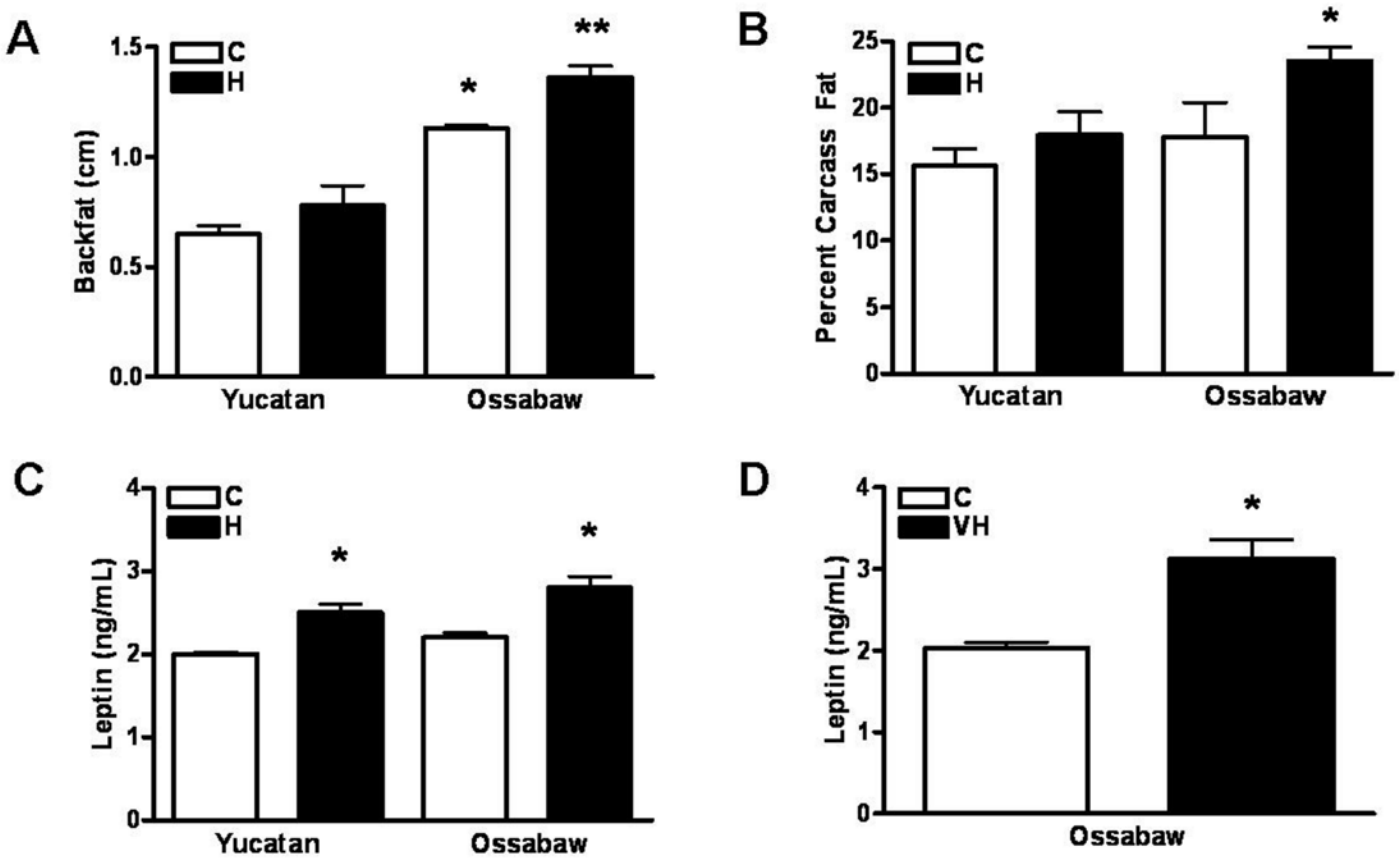

Figure 1. Body fat is greater and leptin increase is blunted in Ossabaw compared with Yucatan swine on calorie-matched diets. (A) Backfat measured by ultrasonography at the fifth rib. *, $P < 0.05$ Ossabaw C versus all other groups; **, $P < 0.05$ Ossabaw H versus all other groups. (B) Percentage of carcass as fat measured by direct chemical analysis. *$P < 0.05$ Ossabaw H versus all other groups. (C) Plasma leptin is increased similarly by H diet in both Ossabaw and Yucatan. *$P < 0.05$ H versus C. (D) Plasma leptin is increased in a subset of Ossabaw fed a very-high–fat (VH) diet consisting of 75% of caloric content from fat. *, $P < 0.05$ Ossabaw C compared with VH.

ameter, 0.014 in.; JoMed, Rancho Cordova, CA) was advanced down the circumflex artery.[61] After angiography-aided placement of the flow wire in a nonbranching section of the circumflex artery, flow velocity signals were allowed to stabilize for several minutes. The analog Doppler signals were digitized continuously both as instantaneous peak velocity and averaged peak velocity

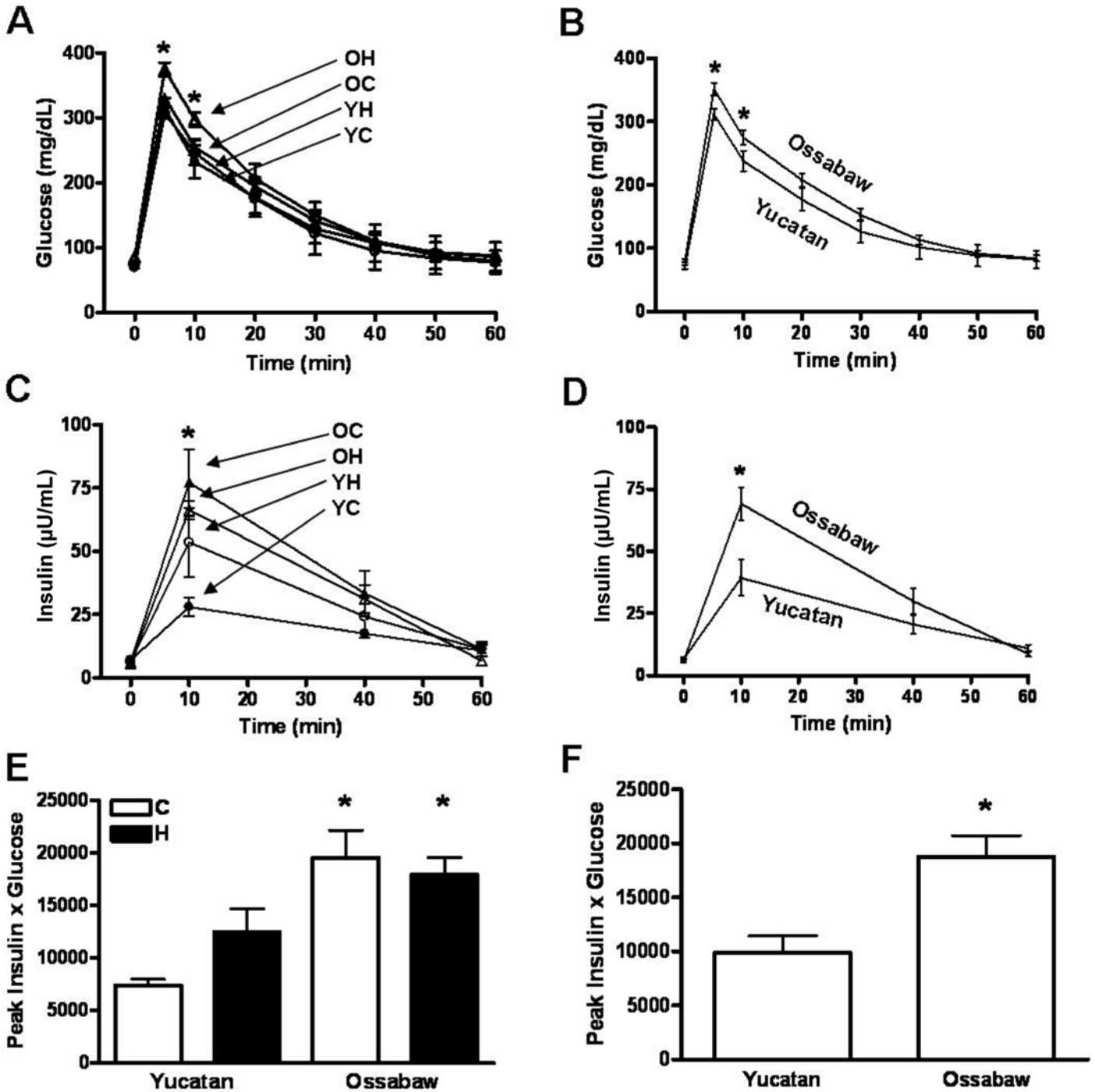

Figure 2. Ossabaw (O) swine are glucose-intolerant and insulin-resistant (hyperinsulinemic) compared with Yucatan (Y) pigs. Intravenous glucose tolerance testing (IVGTT) in Yucatan and Ossabaw swine was initiated by infusion of 0.5 g glucose/kg body weight at time 0. (A) Time course of blood glucose responses in Yucatan control (C, filled circles), Yucatan high-fat–fed (H,open circles), Ossabaw C (filled triangles), and Ossabaw H (open triangles) swine. *, Ossabaw H greater ($P < 0.05$) than all other groups. (B) Data for C and H groups combined by breed to compare glucose levels. (C) Simultaneous measurement of insulin responses during IVGTT. *, all groups greater ($P < 0.05$) than Yucatan C. (D) Data for C and H groups combined by breed to compare insulin levels. (E) Ossabaw C and H swine have greater insulin×glucose values near peak (10 min) during IVGTT than do Yucatan C and H pigs. (F) Combined C and H diets to compare insulin × glucose at peak (10 min).

values. Each average peak velocity value was calculated online as an average of instantaneous peak velocity over 2 consecutive cardiac cycles. All flow data were stored on videotape and personal computer for further offline analysis. Data are shown as coronary flow reserve, which is the adenosine- or bradykinin-induced flow divided by baseline flow velocity. Briefly, baseline flow was defined as 20 to 30 consecutive average peak velocity values (corresponding to approximately 1 min) with less than

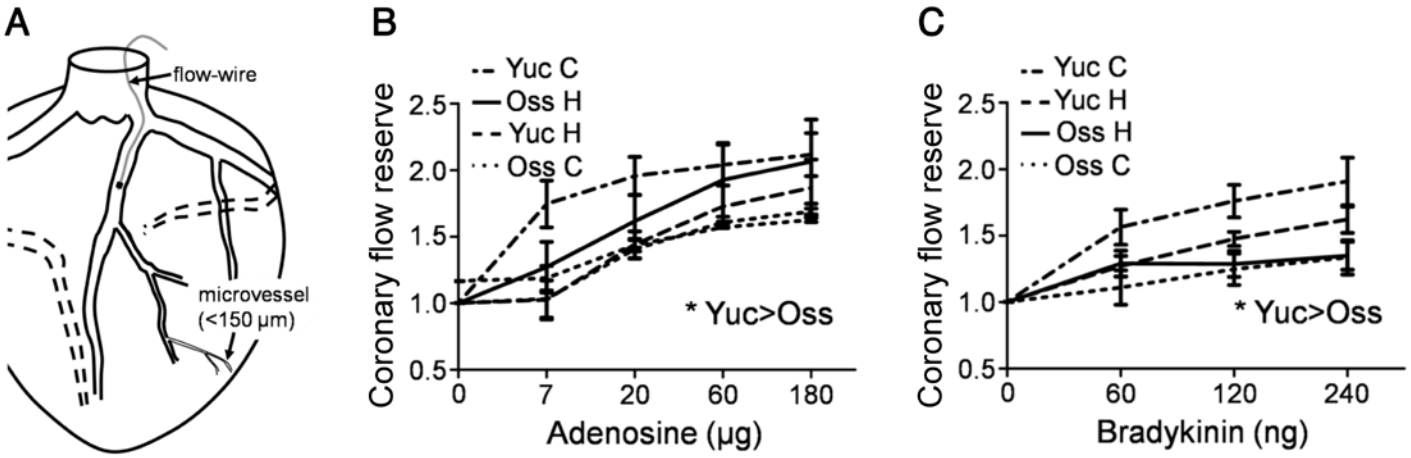

Figure 3. Ossabaw (Oss) swine exhibit coronary microvascular dysfunction compared with Yucatan (Yuc) swine. (A) Coronary schematic illustrates flow wire positioning in circumflex artery (from right anterior oblique view) and downstream microvasculature. (B) Coronary flow reserve is reduced in response to adenosine in Ossabaw swine. C) Ossabaw swine exhibit endothelial dysfunction in response to bradykinin. * $P < 0.05$ by 2-way ANOVA with Bonferroni posttest.

5% variance that were obtained before bolus infusion of adenosine or bradykinin. Adenosine or bradykinin was delivered to the coronary microcirculation by means of bolus infusion through the guiding catheter, as previously described.[61] The peak increase in coronary flow typically occurred within 30 s of the infusion. After each drug bolus, coronary flow was allowed to return to baseline. Saline (vehicle) had no effect on coronary blood flow (data not shown).

Cell dispersion. The procedures for isolation of the nonstented right coronary artery and acute enzymatic dispersal of coronary smooth muscle cells have been described.[32,33,34, 96,97,98] Artery segments (from unstented artery controls and peri-stent sections) were incubated in collagenase solution for 45 min to disperse endothelial cells, followed by a second incubation of 30 min to obtain the smooth muscle cell fraction.

Intracellular Ca^{2+} measurements. Whole-cell intracellular Ca^{2+} levels were measured at room temperature (22 to 25 °C) by using the fluorescent Ca^{2+} indicator fura 2 (InCa++ Ca^{2+} Imaging System, Intracellular Imaging, Cincinnati, OH) as previously described.[32-34, 96-98] Briefly, freshly dispersed cells were incubated with 2.5 µM fura-2–AM (Molecular Probes, Eugene, OR) in a shaking water bath at 37 °C for 20 min before being washed 3 times in a solution containing low Ca^{2+}. An aliquot of cells loaded with fura-2 was placed on a coverslip contained within a constant-flow superfusion chamber that was mounted on an inverted epifluorescent microscope (model TMS-F, Nikon, Melville, NY). Solutions, including those containing 80 mM potassium, caffeine, thapsigargin, and endothelin 1, were superfused at a constant rate of 1 to 2 mL/min. Fura-2 was excited by light from a 300-W xenon arc lamp that was passed through a computer-controlled filter changer containing 340 ± 10 and 380 ± 10 nm bandpass filters. The fluorescence emission at 510 nm was collected by using a monochrome charge-coupled device camera (COHU, San Diego, CA) attached to a 100-MHz Pentium data acquisition computer. Whole-cell fura-2 fluorescence was expressed as the 340:380-nm ratio of fura-2 emission.

Histology. Verhoeff–van Gieson and trichrome staining were performed on sections of stented arteries.[19,55] Neointima formation was determined by obtaining area measurements bounded by the external elastic lamina and internal elastic lamina (tunica media) or internal elastic lamina and lumen (neointima) by using commercially available software (ImagePro 3.0, PowerQuest, Orem, UT). The percentage stenosis was calculated as

% stenosis = area of neointima ÷ (area of tunica media + area of neointima) × 100%.

Collagen content in the sections of the stented arteries was determined by colorimetric analysis of trichrome histology. The adventitia, which is composed predominantly of collagen, was used as the reference color template against which the rest of the section was compared.[15,19]

Assessment of native atheroma. Intravascular ultrasound pullbacks (see *Stent Procedure* in Methods section for details) performed during the stenting procedure before stent placement were used to assess native atheroma. Post-stent evaluations of atheroma were not included in any measure of native atheroma because of the possibility that catheter intervention accelerated atheroma formation. Cross-sectional measurements were obtained every 2 mm through the length of the artery. Each cross-sectional image was divided into 16 equal segments. Percentage wall coverage (by atheroma) was calculated similar to that in previous reports[4,19,51,91] as:

% wall coverage = (no. of segments containing atheroma ÷ 16) × 100%

Statistical analysis. Analyses were performed by using commercially available software (Prism 4.0, GraphPad Software, La Jolla, CA). One-way ANOVA or 2×2 ANOVA with Student–Newman–Keuls or Bonferroni post hoc tests, respectively, were used where appropriate. In all tests, a P value of less than 0.05 was the criterion for statistical significance.

Results

To test the hypothesis that Ossabaw swine were MetS-prone, metabolic profiles were obtained for Ossabaw and Yucatan swine on control and high-fat, atherogenic diets. Regardless of diet, Ossabaw swine had greater body weight and body mass index at euthanasia than did both groups of Yucatan swine, despite

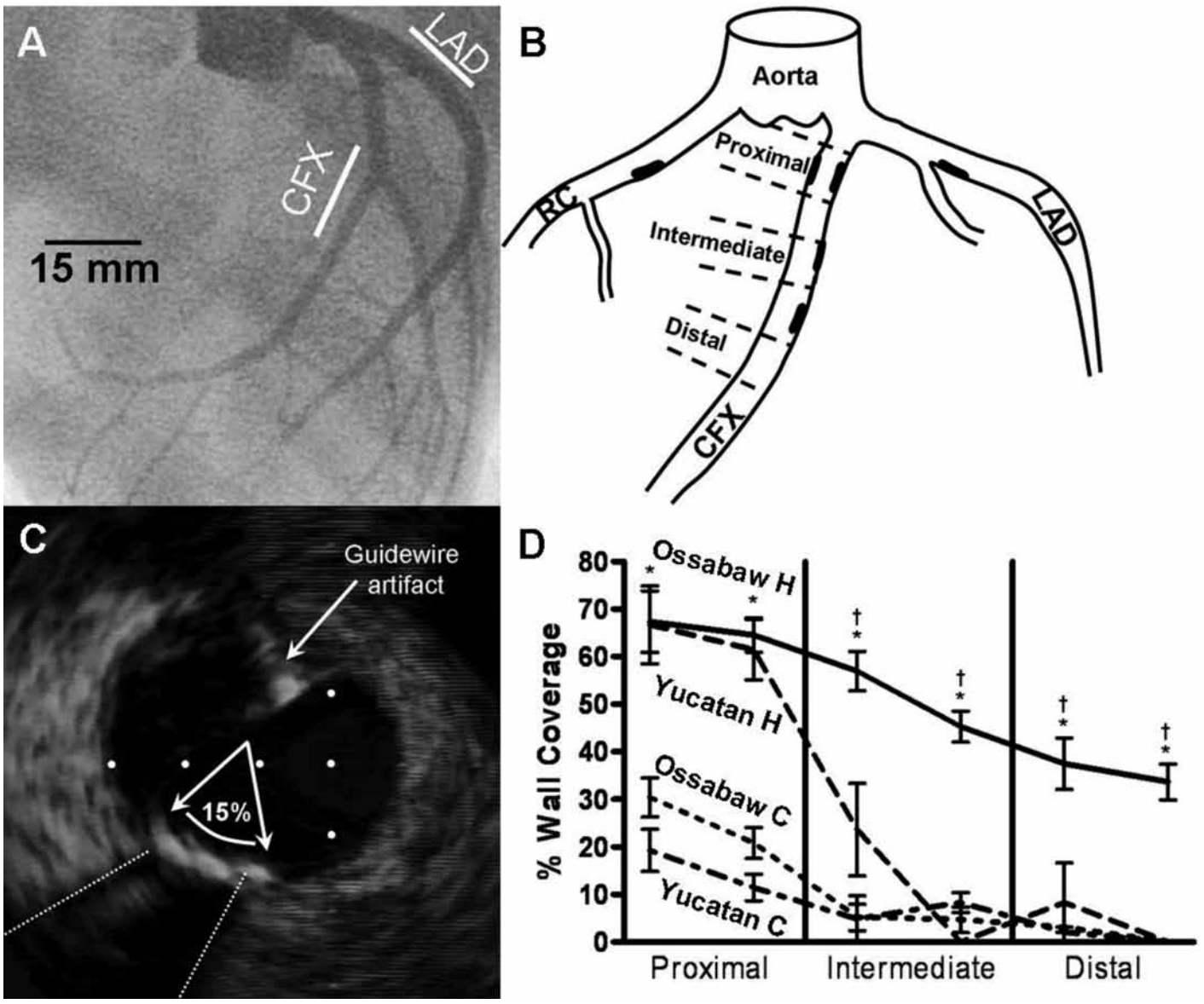

Figure 4. Diffuse atherosclerosis is prominent in Ossabaw compared with Yucatan swine. (A) Angiogram of left coronary arteries, with circumflex (CFX) and left anterior descending (LAD) arteries labeled. (B) The most proximal segment is defined as 0 to 10 mm from the bifurcation of the LAD and CFX arteries. The middle segment (intermediate) is defined as 20 to 30 mm from the bifurcation of the LAD and CFX. The most distal segment is defined as (x – 10) mm to x mm, where x is the most distal measurement of the intravascular ultrasound pullback. The right coronary (RC) artery shown here for completeness is not shown in the angiogram. Image from representative control (C) Ossabaw swine. (C) Intravascular ultrasound image image from high-fat–fed (H) Ossabaw pig showing 15% wall coverage by calcified neointimal formation. Calcification is identified by peripheral signal dropout and is highlighted by dotted lines. (D) Native atheroma (pre-stent) coverage of the artery wall as a percentage of the artery wall area (% wall coverage) is graphed along 3 10-mm segments. Measurements of % wall coverage were taken every 2 mm. *, $P < 0.05$ H compared with C; †, $P < 0.05$ Ossabaw H compared with Yucatan H.

comparable ages and body weights at the start of the study and calorie-matched diets for all groups throughout the study (Table 1). Compared with control diet, hyperlipidemic diet increased total cholesterol, LDL, and HDL levels, although no increases in triglyceride levels were observed (Table 1). Although systolic and diastolic blood pressures showed statistical trends ($P < 0.10$) toward increases in Ossabaw swine, mean arterial pressure was significantly ($P < 0.05$) greater in anesthetized Ossabaw compared with Yucatan swine.

To determine whether increased adipose tissue was responsible for increased body weight and body mass index of Ossabaw swine, back fat was measured by ultrasonography. Ossabaw swine fed the high-fat diet had the most backfat, whereas backfat in Ossabaw swine on the control diet was increased compared to Yucatan swine on either diet (Figure 1 A). Ossabaw swine also demonstrated significantly ($P < 0.05$) greater whole carcass fat as a percentage of body weight, compared with Yucatan swine (Figure 1 B). Concurrently, plasma leptin levels were similar in Ossabaw and Yucatan swine, whereas plasma leptin due to high-fat diet

was increased compared with control diet (Figure 1 C). In a subset of Ossabaw pigs fed a very-high-fat diet containing 75% of total calories from fat, leptin levels were only 55% greater than those in Ossabaw swine on control diet (Figure 1 D).

Both glucose intolerance and insulin resistance are key components of MetS and were assessed in the current study by using IVGTT. Compared with all other groups, Ossabaw swine fed the high-fat diet had significantly ($P < 0.05$) higher blood glucose concentrations at 5 and 10 min after 0.5 mg/kg bolus injection of glucose (Figure 2 A). Further, peak plasma insulin was lower ($P < 0.05$) in control Yucatan swine compared with all other groups. (Figure 2 C). To evaluate the contribution of breed alone on blood glucose and plasma insulin during IVGTT, we combined both diet groups for each pig breed. Ossabaw swine had significantly ($P < 0.05$) greater peak glucose at 5 and 10 min and plasma insulin at 10 min after bolus injection of glucose (Figure 2 B and D). The modified value for homeostatsis model assessment yielded similar results to that of area-under-the-curve measures.[16,52,88] These modified values were significantly ($P < 0.05$) greater in Ossabaw compared with Yucatan swine (Figure 2 E and F).

We assessed coronary microvascular function in Ossabaw and Yucatan swine by measuring blood flow velocity and calculating coronary flow reserve in response to bradykinin and adenosine, 2 well-characterized vasodilators.[61] Placement of the flow wire in the circumflex artery is show in Figure 3 A. Mobilization of coronary flow reserves in response to adenosine was impaired in Ossabaw compared with Yucatan (Figure 3 B). In addition, endothelial cell dysfunction in response to bradykinin was greater in Ossabaw compared with Yucatan pigs (Figure 3 C).

Diffuse atherosclerosis was assessed by measuring neointimal formation in proximal, intermediate, and distal segments of the left anterior descending and circumflex coronary arteries before stent placement, as highlighted in coronary angiograms (Figure 4 A) and diagrams (Figure 4 B). Atheroma was quantified by measuring the percentage of the artery wall with neointimal formation (Figure 4 C), in which a calcified lesion covers 15% of the cross-section of the coronary wall. Atherosclerosis in the proximal segment was increased in Yucatan swine on high-fat diet, but was indistinguishable among these animals and both control groups throughout the intermediate segment. Importantly, atherosclerosis in Ossabaw swine on high-fat diet remained elevated in all segments measured (Figure 4 D), demonstrating that Ossabaw swine develop MetS with diffuse CAD whereas Yucatan swine do not.

In-stent CAD was investigated in Ossabaw and Yucatan swine by evaluating coronary angiograms obtained immediately before stent expansion (Figure 5 A) and during stent expansion with radio-opaque dye within the inflated balloon (Figure 5 B). Verhoeff–Van Gieson elastin (Figure 5 C and D), hematoxylin and eosin (not shown), and trichrome collagen (Figure 5 E and F) stains were used to characterize in-stent CAD and stenosis in Ossabaw and Yucatan swine at 3 wk after stent placement. In-stent neointimal hyperplasia was 2.5-fold greater in Ossabaw compared with Yucatan swine, regardless of diet (Figure 5 G). In addition, Ossabaw swine had more cells per unit area (Figure 5 H) and decreased in-stent collagen content (Figure 5 I) than did Yucatan swine. There was a preponderance of spindle cells (fibroblasts and smooth muscle cells) in the in-stent neointima of Ossabaw compared with Yucatan swine. Therefore, the in-stent neointima of Ossabaw swine was more occlusive, less fibrous, and more cellular than that of Yucatan pigs. Histologic evaluation of the neointima of nonstent artery segments, revealed that the percentage collagen was greater in Yucatan than in Ossabaw swine, with diet having no significant effect (Figure 5 J), whereas cellularity was unchanged (data not shown). CAD in nonstent segments proximal and immediately adjacent to the stent (that is, peri-stent) was quantified by using intravascular ultrasound (Figure 6). Peri-stent CAD was approximately 5-fold greater in Ossabaw compared with Yucatan control pigs, and peri-stent CAD was increased after atherogenic diet in both breeds.

We previously reported that intracellular Ca^{2+} signaling events are altered in coronary arteries with atherosclerotic lesions.[4,9,32,34,61,91,96,98] High extracellular K^+ (that is, 80 mM) depolarized the cell membrane, activating voltage-gated Ca^{2+} channels in CSM, leading to Ca^{2+} influx and a rise in intracellular Ca^{2+} levels (Figure 7 A). In addition, providing high K^+ maximally loaded the Ca^{2+} store of the sarcoplasmic reticulum. The area-under-the-curve of the high-K^+ response did not differ between Yucatan and Ossabaw control animals (Figure 7 B). Subsequent to caffeine-induced Ca^{2+} release from the sarcoplasmmic reticulum, intracellular Ca^{2+} levels rose transiently then fell over time due to Ca^{2+} extrusion (efflux) and sequestration mechanisms (Figure 7 A). Baseline-subtracted peak Ca^{2+} response to caffeine (5 mM) was not different between Yucatan C and Ossabaw control swine (Figure 7 C). Overall buffering of intracellular Ca^{2+} was measured as time from peak Ca^{2+} response to caffeine to half the initial baseline (that is, half minimum). CSM from Ossabaw control pigs in Ca^{2+}-containing and Ca^{2+}-free solution displayed increased time to half minimum from peak Ca^{2+} response to caffeine compared with CSM from Yucatan controls (Figure 7 D), thus providing evidence for decreased Ca^{2+} efflux in Ossabaw compared with Yucatan control swine.

In addition, CSM from peri-stent and nonstent arterial segments of Yucatan and Ossabaw control and high-fat–fed swine were assessed for sarco–endoplasmic reticulum Ca^{2+} ATPase (SERCA) function. CSM were depolarized with high K^+ to load the sarcoplasmic reticulum (Figure 8 A). Endothelin 1 (ET1, 30 nM) elicited release of Ca^{2+} from the sarcoplasmic reticulum, whereas thapsigargin (1 μM) prevented Ca^{2+} uptake into the sarcoplasmic reticulum by blocking SERCA. SERCA buffering of Ca^{2+} was assessed by the effect of full SERCA inhibition by thapsigargin on the peak Ca^{2+} response to ET1. SERCA buffering of Ca^{2+} was not involved in the overall Ca^{2+} response to ET1 in Yucatan C in either peri- or nonstent CSM (Figure 8 B and C). In contrast, SERCA contributed significantly to buffering the ET1-associated Ca^{2+} response in nonstent CSM from high-fat–fed Yucatan swine, as evidenced by increased peak Ca^{2+} response to ET1 after thapsigargin treatment (Figure 8 D). In other words, SERCA function was increased in native atherosclerotic arterial segments. Importantly, peri-stent CSM from high-fat–fed Yucatan swine have SERCA dysfunction, because their peak Ca^{2+} response to ET1 is similar to that of non- and peri-stent CSM, in which SERCA was inhibited completely by thapsigargin treatment. CSM from both non- and peri-stent segments from Ossabaw control swine had increased SERCA function, as evidenced by increased peak Ca^{2+} response to ET1 in the presence of thapsigargin (Figure 8 E). SERCA function is virtually nonexistent in CSM from non- and peri-stent segments from high-fat–fed Ossabaw swine, in that peak Ca^{2+} response to ET1 was elevated in the absence of thapsigargin (Figure 8 F). Therefore, buffering of the peak Ca^{2+} response

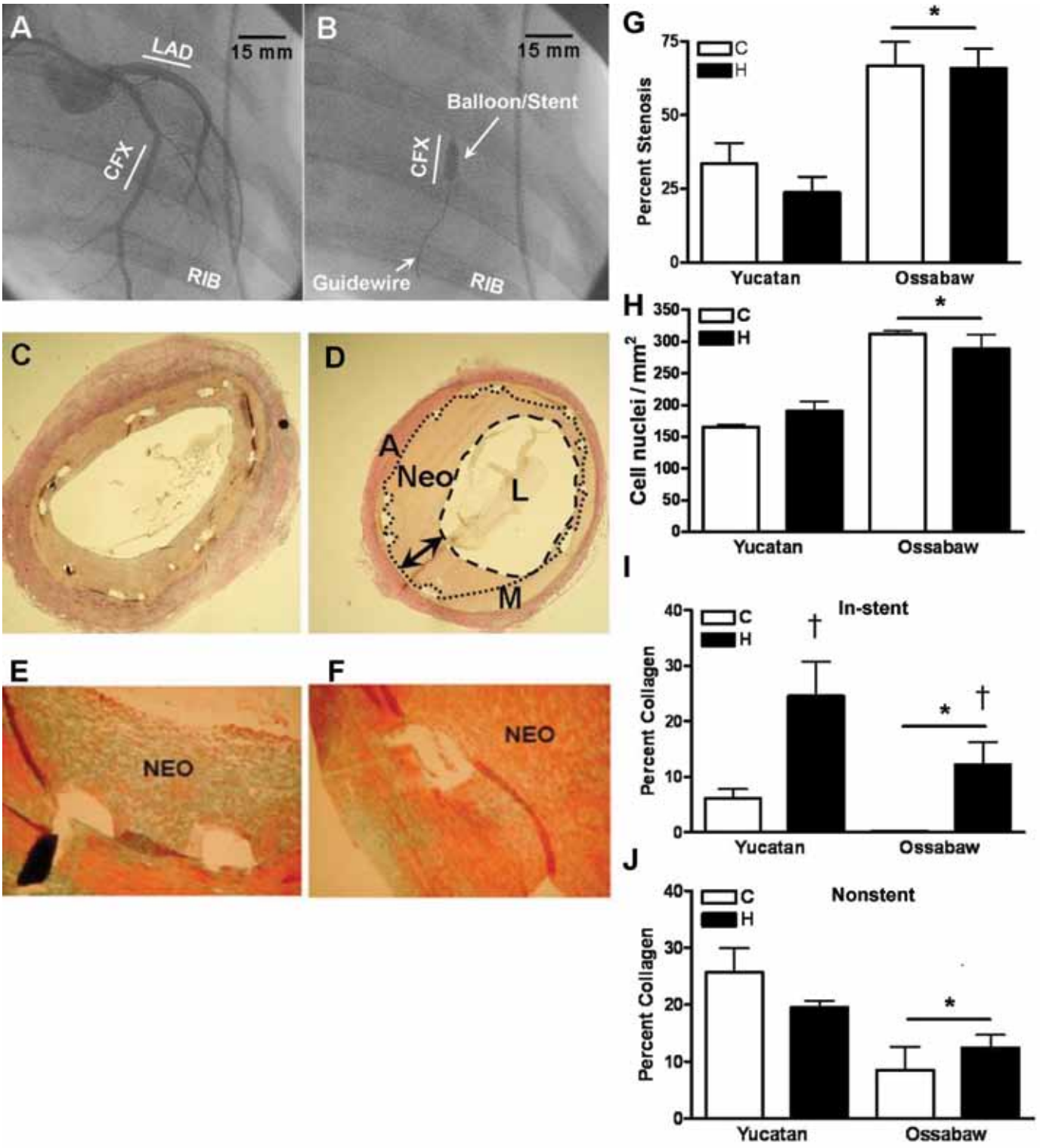

Figure 5. In-stent stenosis is greater in Ossabaw compared with Yucatan swine. Coronary angiogram in right anterior oblique 30° view (A) prior to and (B) during stent deployment in a representative control (C) Yucatan pig. (C) Representative Verhoeff–Van Gieson stain of Yucatan C in-stent CAD. D) Representative Verhoeff–Van Gieson stain of Ossabaw C in-stent CAD illustrating adventitia (A), neointima (Neo), media (M), lumen (L), and pre-stent lumen border (dotted line) and post-stent lumen border (dashed line) of neointimal hyperplasia. (E and F) Histology using Masson trichrome collagen staining (blue). Open spaces to the left and below neointima are from stent struts that were removed in sectioning. (G) Percentage cross-sectional area of stenosis calculated by histology is greater in Ossabaw C and H than Yucatan C and H, with no effect of atherogenic diet (H). (H) Ossabaw C and H swine have greater cell nuclei per unit area than do Yucatan C and H swine. Percentage collagen in neointima area of (I) in-stent and (J) nonstent artery segment. *, $P < 0.05$ Ossabaw compared with Yucatan; †, $P < 0.05$ C compared with H diet.

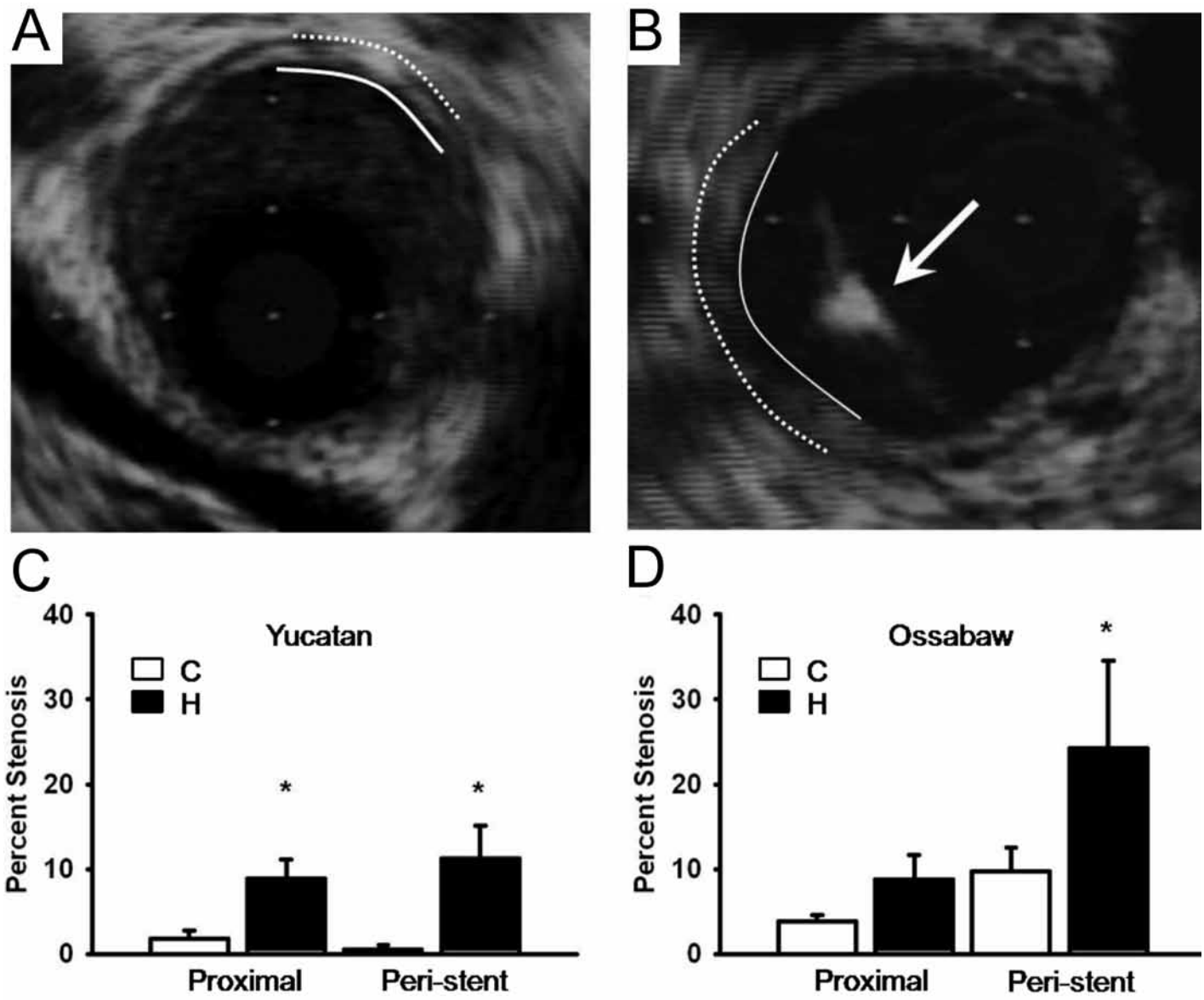

Figure 6. Peri-stent CAD is greater in Ossabaw compared with Yucatan swine, and hyperlipidemia increases proximal peri- and nonstent CAD. Representative intravascular ultrasound (IVUS) images of (A) Yucatan and (B) Ossabaw (B) peri-stent CAD. Lumen/neointima (solid line) and neointima/media (dotted line) were used to calculate neointimal area and percent stentosis. White arrow in panel B illustrates IVUS guidewire artifact. (C) Hyperlipidemia increases both proximal nonstent and peri-stent CAD in Yucatan swine. (D) Peri-stent disease is increased in high-fat–fed (H) compared with control (C) Ossabaw swine and compared with respective Yucatan C and H pigs. Group differences assessed by 2-way ANOVA with Bonferroni post hoc analysis.

to ET1 transitions from increased SERCA function in mild CAD to decreased SERCA function in moderate to severe CAD.

Discussion

The major findings of the current study are that compared with Yucatan pigs, Ossabaw swine have 1) greater elevations in 4 metabolic features of MetS; 2) coronary microvascular dysfunction in response to adenosine (primarily mediated by smooth muscle) and bradykinin (endothelium-mediated); 3) greater native atheroma, diffuse atheroma, in-stent neointimal hyperplasia, and peri-stent atheroma; 4) less fibrous and more cellular atherosclerotic lesions within nonstented and stented segments of coronary artery, and 5) impaired coronary smooth muscle intracellular Ca^{2+} buffering and efflux after Ca^{2+} release from the sarcoplasmic reticulum. This study is the first to directly compare multiple symptoms of the MetS, CAD, and in-stent restenosis between Ossabaw and Yucatan swine fed calorie-matched control chow and high-fat, high-cholesterol atherogenic diet.

Phenomenal work has been done on transgenic and gene ablation (knockout) mouse models (for example, reference 60) and summarized recently by the Animal Models of Diabetic Complications Consortium[36] to understand mechanisms of obesity and MetS. However, transgenic mouse models simply are inadequate for vascular interventions using stents identical to those used in

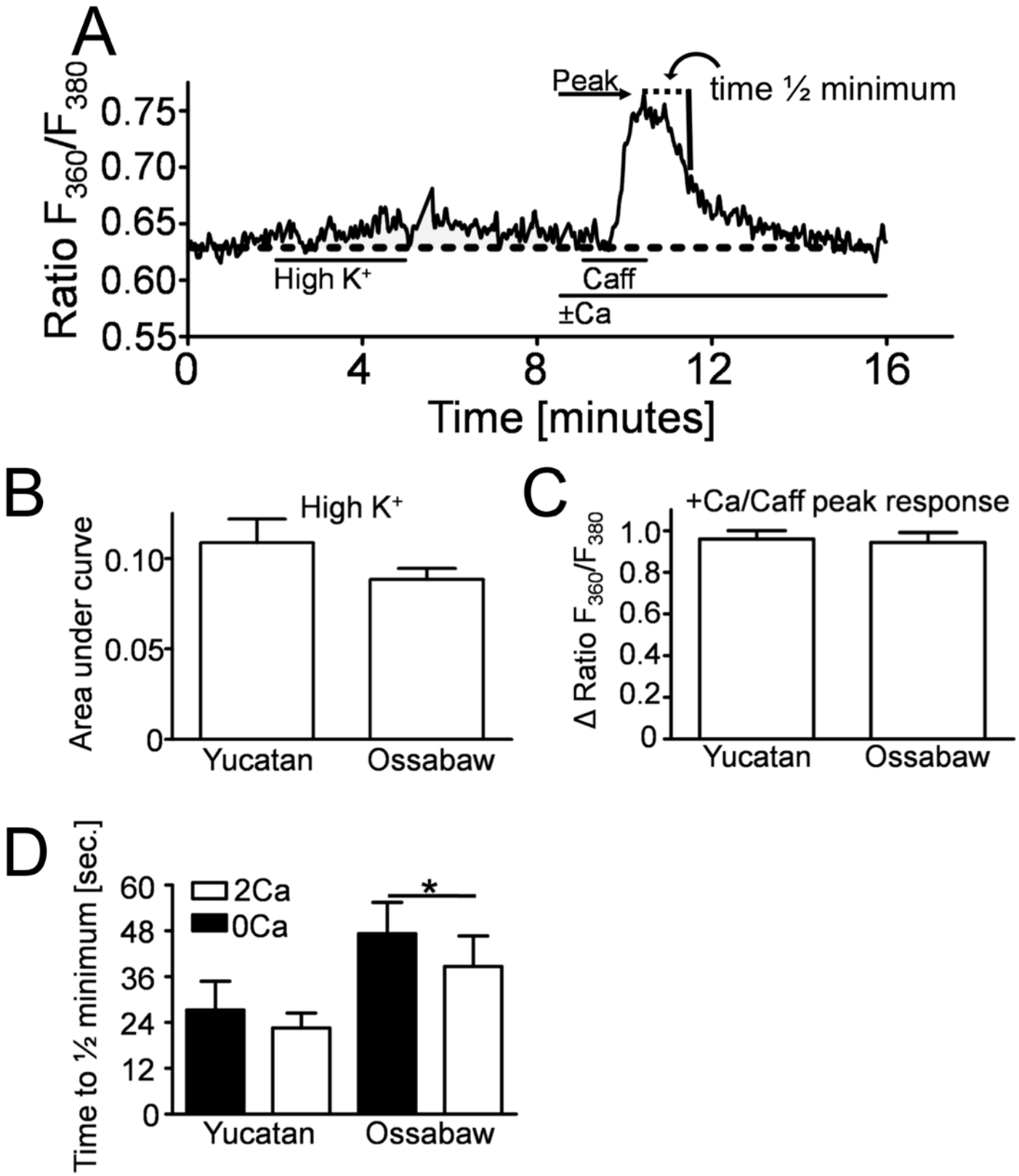

Figure 7. Dysfunctional Ca^{2+} efflux in CSM from Ossabaw compared to CSM from Yucatan. (A) Duration of exposure to solutions is shown by horizontal lines. Representative Ca^{2+} tracing (fura-2 ratio) demonstrates Ca^{2+} influx response to 80 mM K^+ depolarizing solution (High K^+), peak Ca^{2+} response to caffeine (Caff, 5 mM), and time to half minimum from caffeine-induced Ca^{2+} peaks. (B) Integral of the intracellular Ca^{2+} response to depolarizing solution is not different between CSM from control (C) Ossabaw and Yucatan swine. (C) Peak Ca^{2+} response to caffeine is not different between CSM from C Ossabaw and Yucatan swine. (D) Time to half minimum from peak is increased in CSM from C Ossabaw compared with Yucatan.

humans,[18,23,38,55,57,79,83,86] a step that is essential for translation to the clinic. Because the Ossabaw miniature swine model of MetS also develops mature, clinically significant atheroma that includes the presence of lipid cores, foam cells, proliferating smooth muscle cells, and small foci of calcification,[42,92] it has the potential to yield vastly superior information than that gained through other stenting studies that involved injury of healthy arteries.[38,57,79,86]

A primary advantage of Ossabaw miniature swine use in research is their predisposition to obesity, natural occurrence of MetS, and progression to type 2 diabetes, which is unique to Ossabaw swine. Table 2 compares the major features of MetS in Yucatan and Ossabaw miniature swine and their utility as cardiovascular disease models and for study of Ca^{2+} signaling. Yucatan pigs are our comparison because of our extensive work with this genetically leaner pig, which is the predominantly used miniature swine for laboratory research. The current study yielded relatively mild differences in various metabolic parameters (for example, body mass index, hyperglycemia, hyperinsulinemia, and hypercholesterolemia) after atherogenic diet feeding, compared with previous reports in Ossabaw and Yucatan swine (summarized in Table 2). This outcome was a direct result of our study's aim to sensitively measure breed differences by calorie-matching control and high-fat diets to that required for maintenance of normal body weight in adult Yucatan swine, rather than by inducing maximal MetS by overfeeding the high-fat groups. Rigorous comparison revealed the much greater propensity to obesity (that is, 'thriftiness') of Ossabaw compared with Yucatan swine. High-fat–fed Ossabaw swine demonstrated increased back and carcass fat compared with breed controls, but Yucatan swine lacked similar differences between high-fat–fed and control groups (Figure 1 A and B).

Leptin insensitivity leads to ectopic lipid accumulation, in turn contributing to insulin insensitivity.[56] Although backfat and carcass fat were greater in high-fat–fed Ossabaw than Yucatan swine, plasma leptin was similarly and modestly elevated in both high-fat–fed Ossabaw and Yucatan pigs compared with their respective controls. Lending support to this finding are our previously published data,[95] which revealed that leptin levels in hypercaloric high-fat–fed Yucatan swine were 84% greater than those of high-fat–fed Yucatan swine in the current study (Figure 1 C). In contrast, hypercaloric very-high-fat–fed Ossabaw swine displayed only an 11% increase in plasma leptin over that in high-fat–fed Ossabaw (Figure 1 C and D), although the hypercaloric swine were much more obese (data not shown). This result suggests that Ossabaw pigs have a deficient (blunted) leptin response to increased adipose, and this dampening may explain in part the increased weight gain that contributes to MetS in these pigs, a situation strikingly similar to the constellation of leptin deficiency, obesity, and MetS in humans.[21] In summary, Ossabaw swine clearly show greater propensity to obesity than do Yucatans and direct measures show a greater accumulation of visceral fat on rigorously controlled experimental diets (Figure 1B).

Type 2 diabetes has been defined in humans as a fasting blood glucose exceeding 126 mg/dL. Perhaps less known is that the fasting blood glucose in healthy adults is approximately 90 mg/dL (range, 74 to 110 mg/dL).[78] Therefore, an approximate 1.4-fold increase in the fasting blood glucose level in humans renders a diagnosis of diabetes mellitus. Given this information, our laboratory has several publications demonstrating increased fasting blood glucose on the order of 1.4-fold,[9] 1.7-fold,[5] 1.4-fold,[7] and 2.2-fold[6] in swine demonstrating MetS. Although similar to humans, glucose homeostasis in swine shows important differences that should be taken into careful consideration when defining diabetes in swine.[44] Chief among these concerns are the lower fasting glucose levels (60 to 80 mg/dL[47]) in healthy swine compared with humans. Also of importance is that swine have relatively high glucose tolerance to oral glucose load and increased clearance after intravenous glucose load.[44] In addition, pancreatic β-cell:body mass ratio in swine is twice that in humans, suggesting considerable insulin secretory reserve in swine.[49,58] Taken together, these observations suggest that lower thresholds for the diagnosis of prediabetes and diabetes mellitus should be considered for swine.

Despite intensive efforts to induce insulin resistance and glucose intolerance in Yucatan swine on high-fat, high-cholesterol, and high-sucrose diets, we have found that currently available Yucatan pigs do not naturally develop obesity-associated insulin resistance[68,70,72,73] (Table 2). In contrast, Ossabaw swine fed a high-calorie diet display natural pathogenesis of MetS with hyperinsulinemia and eventual progression to type 2 diabetes as evidenced by a significantly increased fasting blood glucose.[5,6,7,9] Other miniature swine breeds currently available for laboratory animal medicine (that is, Yucatan and Gottingen) do not progress to type 2 diabetes,[45,68,72] although Gottingen pigs will develop mild MetS.[43,45,46,48] Despite outstanding work showing that a line of crossbred domestic pigs with familial hypercholesterolemia develop MetS,[3] the use of standard-size domestic swine is impractical because they weigh more than 250 kg and are 2 y old before type 2 diabetes occurs. Furthermore, a 250-kg pig is not amenable to the use of the conventional angiography instrumentation needed for stent deployment, compared with the convenient small stature of Ossabaw miniature swine (Table 2).

Dyslipidemia was comparable between Yucatan and Ossabaw swine in the present study (Table 1), but other studies using hypercaloric diets showed robust increases in LDL:HDL and triglycerides in Ossabaw swine (Table 2). The similar dyslipidemia but greater and diffuse CAD in MetS Ossabaw compared with Yucatan pigs clearly indicates that CAD is not driven simply by increased cholesterol levels.[36] Instead, the addition of more components of MetS (for example, obesity) likely may exacerbate hyperlipidemia-induced CAD. Genetically leaner Yucatan pigs made mildly obese and hyperlipidemic by consumption of excess calorie atherogenic diet did not become hypertensive[8,68,96] (Table 1). In contrast, in all of our chronic studies of hypercaloric feeding of Ossabaw swine, hypertension was a clear finding (Table 2), thus indicating MetS. Convincing evidence of 'obesity hypertension'[30] is the robust, 5-fold increases in plasma renin and aldosterone in Ossabaw swine.[1]

In the current study, we show that mild MetS in Ossabaw swine increases CAD. Although high-fat–fed Ossabaw and Yucatan swine have similar levels of CAD in proximal arterial segments, high-fat–fed Ossabaw pigs—the only group to exhibit elevated peak glucose in response to glucose tolerance testing—have diffuse atherosclerosis, a hallmark of patients with diabetes[64,65,67] (Table 2). This difference in CAD between Yucatan and Ossabaw swine is especially striking considering the modest metabolic differences.

Patients with MetS have increased incidence of CAD,[27] and those presenting with flow-limiting coronary occlusions are treated primarily by stent deployment. Drug-eluting stents have

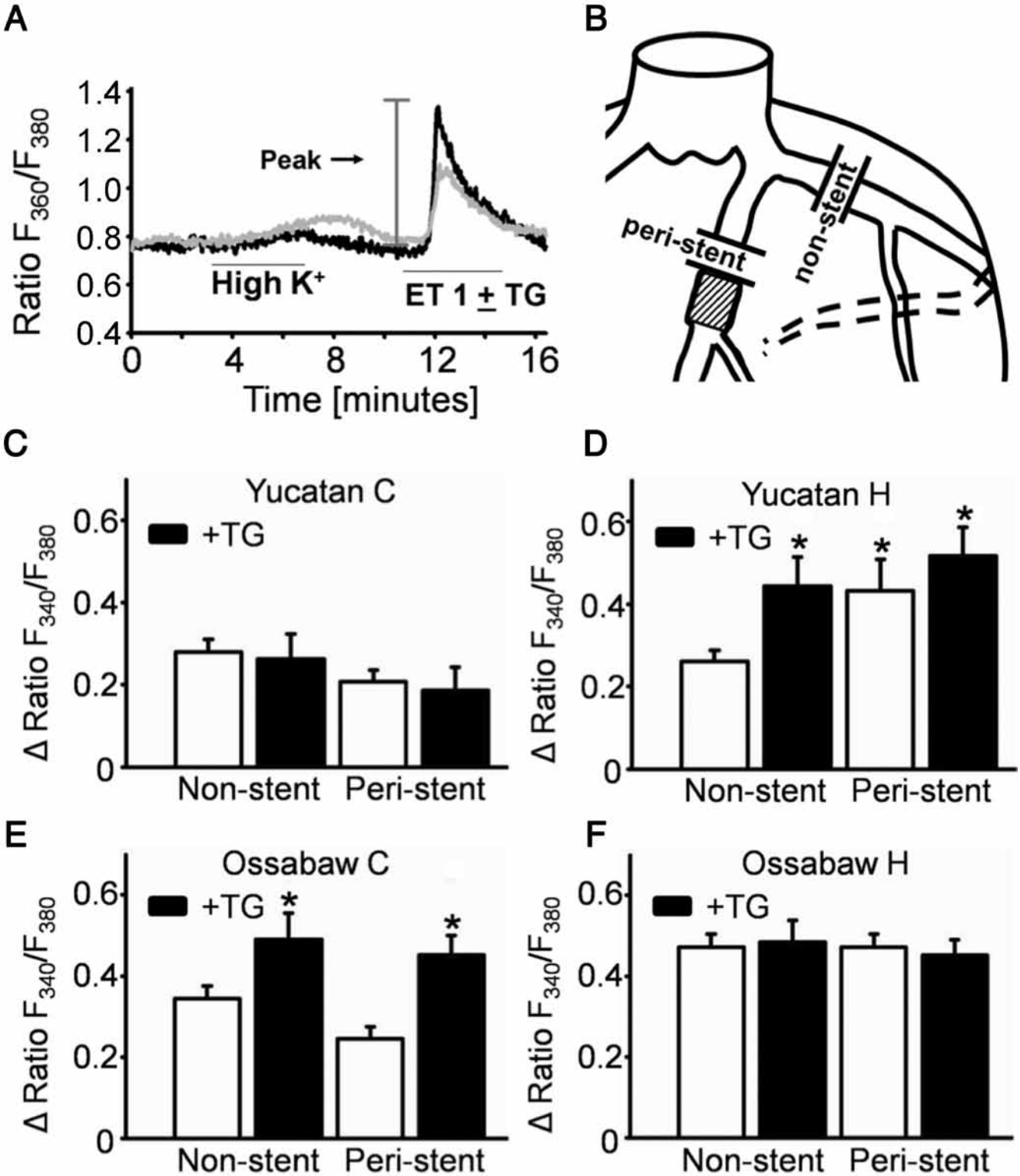

Figure 8. SERCA Ca^{2+} modulating function progresses from increased function to virtually complete dysfunction with severity of CAD. (A) Duration of exposure to solutions is shown by horizontal lines. Representative Ca^{2+} tracing (fura-2 ratio) demonstrates Ca^{2+} influx response to 80 mM K^+ depolarizing solution (High K^+) and peak Ca^{2+} response to endothelin 1 (ET1, 30 nM) in CSM cells in the presence (black tracing; black bars, C through F) or absence (gray tracing; white bars, C through F) of thapsigargin (TG; 1 μM). (B) Coronary artery schematic illustrates non- and peri-stent segments from which CSM cells were dispersed. (C) SERCA function does not alter peak Ca^{2+} response to caffeine in CSM from lean, healthy Yucatan control (C) swine. (D) Thapsigargin inhibition of SERCA in CSM from peri- and nonstent segments of high-fat–fed (H) Yucatan swine revealed an increased role of SERCA in attenuating the ET1-induced increase in intracellular Ca^{2+}. (E) SERCA attenuates peak Ca^{2+} response to ET1 in CSM from C Ossabaw. (F) SERCA function is inhibited in CSM from H Ossabaw.

Table 2. Comparison of MetS (items 1 through 6) in Yucatan (Y) and Ossabaw (O) miniature swine, utility as cardiovascular disease models (items 7 and 8), and cellular or molecular characteristics (items 9 through 12)

Characteristic	Yucatan	Ossabaw	References
1. Obesity	No	O > Y	4, 8, 9, 16, 20, 52, 83, 95; Table 1; Figure 1
2. Insulin resistance	No	Yes	16, 19, 52, 68, 83, 96; Figure 2
3. Glucose intolerance (or impaired glucose tolerance)	No	Yes	4, 8, 9, 15, 16, 19, 52, 62, 68, 83, 95, 96, 98; Figure 2
4. Dyslipidemia (increased LDL:HDL or LDL:total cholesterol)	Yes	Yes	9, 15, 16, 19, 51, 52, 77, 83, 98; Table 1
5. Dyslipidemia (increased triglycerides)	No	Yes	9, 15, 16, 19, 34, 52, 62, 77, 83, 95, 96
6. Hypertension	No	Yes	9, 16, 19, 68, 80, 83
7. Cardiovascular disease, atherosclerosis	Yes	Yes	4, 5, 6, 7, 9, 15, 16, 18, 19, 29, 39, 40, 42, 50, 55, 61, 62, 83, 87, 91, 92; Figures 3 through 6
8. Small stature	Yes	Yes	8, 9, 16, 83, 95; Table 1
9. Other (for example, vascular calcification, AMP kinase alleles)	No	Yes	42, 54, 66, 92; Figure 3
10. CSM Ca^{2+} efflux dysfunction	Yes	O > Y	96, 98; Figure 7
11. CSM SERCA dysfunction	Yes	O > Y	32, 34, 98; Figure 8
12. CSM store-operated Ca^{2+} entry	No	Yes	14, 19, 31

greatly reduced restenosis rates, but restenosis remains a major concern when treatment is complicated by diffuse and severe atheroma, which progresses much more aggressively in regions adjacent to the stent (so-called 'peri-stent CAD').[64,65,67] Ossabaw swine, which show at least 6 features of MetS (Table 2), have increased peri- and in-stent CAD (Figures 5 and 6), compared with Yucatan swine. Interestingly, pig breed, but not diet, is associated with increased in-stent stenosis. This outcome differs from that of nonstent segments, in which only the combination of the Ossabaw breed and atherogenic diet elicited diffuse atherosclerosis. These findings suggest that factors key to CAD in Ossabaw swine drive their greater peri- and in-stent CAD compared with that in Yucatan swine; possible factors include: 1) components of MetS not examined in our study, 2) other inflammatory mediators, and 3) genetic components beyond the thrifty genotype (for example, vascular wall differences) that render coronary arteries more sensitive to stenting. The most likely difference, however, is hyperinsulinemia, which was present in Ossabaw compared with Yucatan swine. Although some reports indicate no greater coronary restenosis in patients with MetS compared to healthy patients,[76] considerable evidence supports a role for the hyperinsulinemia component of MetS in increased restenosis after percutaneous coronary interventions.[74,75,84,85] Particularly compelling is a study[84] showing serial intravascular ultrasound measures of coronary restenosis in humans.

Mechanisms underlying CAD and vascular response to injury are not completely understood, but we and others have reported that altered CSM Ca^{2+} signaling is involved in diabetic CAD.[9,19,32,34,41,51,91,96,98] Intracellular free Ca^{2+} concentration is determined by 3 major mechanisms: Ca^{2+} influx, Ca^{2+} extrusion, and intracellular Ca^{2+} sequestration by the sarcoplasmic reticulum. Important observations in the present study include no difference in Ca^{2+} influx in response to depolarizing extracellular solution (Figure 7 B; quantifies mainly voltage-gated Ca^{2+} channel activity in the plasma membrane[34,98]) or peak Ca^{2+} in response to caffeine treatment (Figure 7 C; quantifies Ca^{2+} stores in the sarcoplasmic reticulum[81,82,97]) between Ossabaw and Yucatan swine. In the presence and absence of extracellular Ca^{2+}, increased time to half minimum in response to caffeine indicates decreased Ca^{2+} extrusion across the plasma membrane (Ca^{2+} efflux[97,98]) in CSM from Ossabaw compared with Yucatan swine (Figure 7 D). Importantly there was no difference in time to half minimum despite the presence or absence of extracellular Ca^{2+} for CSM from either breed (Figure 7D), suggesting store-operated Ca2+ entry (SOCE) was not a predominant factor.

The lack of SOCE in Ossabaw CSM may appear to contradict recently published results from our laboratory implicating the SOCE channel transient receptor potential classical 1 (TRPC1) in MetS- and stent-induced CAD in Ossabaw swine.[19] However, an important difference between the previous and current studies is the induction of robust MetS and severe CAD of the earlier work compared with the relatively mild MetS and CAD induced here. The current finding that SOCE is not evident in CSM from Yucatan swine confirms previous reports by our laboratory,[14,31] although we have observed robust SOCE in endothelial cells.[25] Interestingly, SERCA does not influence the peak response to ET1 in CSM from non- and peri-stent segments from Yucatan pigs fed the control diet (Figure 8 C). The Ca^{2+} response is maintained at normal levels with increased SERCA function in CSM from both non- and peri-stent Ossabaw controls (Figure 8 E), compared with Yucatan controls. SERCA function increases with maintenance of peak response in CSM from nonstent segments from high-fat–fed compared with control Yucatan, but high-fat–fed Yucatan peri-stent CSM are unable to maintain peak response despite increased SERCA function (Figure 8 D). Incredibly, SERCA is virtually nonfunctional in CSM from non- and peri-stent sections of high-fat–fed Ossabaw swine (Figure 8 F), as assessed by peak response to ET1 with or without thapsigargin.

Complex and unstable plaque formation lead to increased risk of thrombosis,[13] resulting in acute myocardial infarction. We have observed more than 500 Yucatan coronary arteries without documenting calcified coronary lesions; however, Ossabaw coronary arteries contain calcified lesions (Figure 3 C, Table 2). Previously published data demonstrated collagen-rich atherosclerotic tissue in restenotic specimens was greater in humans with diabetes than in nondiabetic patients.[63] In contrast, we show an approximate 2-fold increase in percentage collagen of in-stent segments in high-fat–fed Yucatan swine compared to high-fat–fed Ossabaw swine. One possible explanation is that the atherosclerotic tissue in the human study is more mature, whereas that in our study is at an early stage of progression, which is characterized by less stable plaque formation. The complex (highly cellular, calcified,

and less fibrous) neointimal composition observed in stented segments of Ossabaw coronary artery suggests a complex, mature, proliferative, or lipid-laden composition, which is thus potentially more vulnerable to plaque rupture.

Ossabaw swine were first used as a laboratory animal model almost 40 y ago[59] and may be more relevant now than ever due to the increasing incidence of MetS and type 2 diabetes in Western society.[94] Ossabaw swine remarkably mimic the MetS and advanced CAD seen in humans and likely will serve as an excellent large animal model for the study of metabolic abnormalities and CAD in the future.

Acknowledgments

We thank the many outstanding coworkers who contributed to this work, especially J Bryd, J Wenzel, R Boullion, and Dr C A Witczak. We thank J M Sturek for initial strategies for segmental analysis of intravascular ultrasound images to characterize diffuse coronary artery disease. This work was supported by the National Institutes of Health grant numbers HL062552 and RR013223 and an Innovation Award from the American Diabetes Association (to MS), the Purdue–Indiana University Comparative Medicine Program, and the Fortune–Fry Ultrasound Research Fund of the Department of Cellular and Integrative Physiology at Indiana University School of Medicine. JME and ZPN are recipients of a Translational Research Fellowship from the Indiana University School of Medicine, ZPN was the recipient of a Translational Fellowship from NIH UL1 RR025761, and XL was the recipient of a Predoctoral Fellowship from the American Heart Association.

References

1. **Alloosh M, Pratt JH, Sturek M, Basile DP**. 2008. Elevated renin and enhanced adrenal steroidogenesis in the Ossabaw miniature swine model of the metabolic syndrome. FASEB J **22:**736.7.
2. **AVMA Panel on Euthanasia. American Veterinary Medical Association.** 2001. 2000 Report of the AVMA panel on euthanasia. J Am Vet Med Assoc **218:**669–696.
3. **Bellinger DA, Merricks EP, Nichols TC.** 2006. Swine models of type 2 diabetes mellitus: insulin resistance, glucose tolerance, and cardiovascular complications. ILAR J **47:**243–258.
4. **Bender SB, Tune JD, Borbouse L, Long X, Sturek M, Laughlin MH.** 2009. Altered mechanism of adenosine-induced coronary arteriolar dilation in early-stage metabolic syndrome. Exp Biol Med (Maywood) **234:**683–692.
5. **Borbouse L, Dick GM, Asano S, Bender SB, Dincer UD, Payne GA, Neeb ZP, Bratz IN, Sturek M, Tune JD.** 2009. Impaired function of coronary BK_{Ca} channels in metabolic syndrome. Am J Physiol Heart Circ Physiol **297:**H1629–H1637.
6. **Borbouse L, Dick GM, Payne GA, Berwick ZC, Neeb ZP, Alloosh M, Bratz IN, Sturek M, Tune JD.** 2010. Metabolic syndrome reduces the contribution of K^+ channels to ischemic coronary vasodilation. Am J Physiol Heart Circ Physiol **298:**H1182–H1189.
7. **Borbouse L, Dick GM, Payne GA, Payne BD, Svendsen MC, Neeb ZP, Alloosh M, Bratz IN, Sturek M, Tune JD.** 2010. Contribution of BK_{Ca} channels to local metabolic coronary vasodilation: effects of metabolic syndrome. Am J Physiol Heart Circ Physiol **298:**H966–H973.
8. **Boullion RD, Mokelke EA, Wamhoff BR, Otis CR, Wenzel J, Dixon JL, Sturek M.** 2003. Porcine model of diabetic dyslipidemia: insulin and feed algorithms for mimicking diabetes in humans. Comp Med **53:**42–52.
9. **Bratz IN, Dick GM, Tune JD, Edwards JM, Neeb ZP, Dincer UD, Sturek M.** 2008. Impaired capsaicin-induced relaxation of coronary arteries in a porcine model of the metabolic syndrome. Am J Physiol Heart Circ Physiol **294:**H2489–H2496.
10. **Camici PG, Crea F.** 2007. Coronary microvascular dysfunction. N Engl J Med **356:**830–840.
11. **Carroll JA, Daniel JA, Keisler DH, Matteri RL.** 1999. Nonsurgical catheterization of the jugular vein in young pigs. Lab Anim **33:**129–134.
12. **Christoffersen BO, Grand N, Golozoubova V, Svendsen O, Raun K.** 2007. Gender-associated differences in metabolic syndrome-related parameters in Gottingen minipigs. Comp Med **57:**493–504.
13. **Daemen J, Wenaweser P, Tsuchida K, Abrecht L, Vaina S, Morger C, Kukreja N, Juni P, Sianos G, Hellige G, Van Domburg RT, Hess OM, Boersma E, Meier B, Windecker S, Serruys PW.** 2007. Early and late coronary stent thrombosis of sirolimus-eluting and paclitaxel-eluting stents in routine clinical practice: data from a large 2-institutional cohort study. Lancet **369:**667–678.
14. **Dick GM, Sturek M.** 1996. Effects of a physiological insulin concentration on the endothelin-sensitive Ca^{2+} store in porcine coronary artery smooth muscle. Diabetes **45:**876–880.
15. **Dixon JL, Shen S, Vuchetich JP, Wysocka E, Sun G, Sturek M.** 2002. Increased atherosclerosis in diabetic dyslipidemic swine: protection by atorvastatin involves decreased VLDL triglycerides but minimal effects on the lipoprotein profile. J Lipid Res **43:**1618–1629.
16. **Dyson MC, Alloosh M, Vuchetich JP, Mokelke EA, Sturek M.** 2006. Components of metabolic syndrome and coronary artery disease in female Ossabaw swine fed excess atherogenic diet. Comp Med **56:**35–45.
17. **Eckel RH, Kahn R, Robertson RM, Rizza RA.** 2006. Preventing cardiovascular disease and diabetes: a call to action from the American Diabetes Association and the American Heart Association. Circulation **113:**2943–2946.
18. **Edwards JM, Alloosh M, Long X, Dick GM, Lloyd PG, Mokelke EA, Sturek M.** 2008. Adenosine A_1 receptors in neointimal hyperplasia and in-stent stenosis in Ossabaw miniature swine. Coron Artery Dis **19:**27–31.
19. **Edwards JM, Neeb ZP, Alloosh MA, Long X, Bratz IN, Peller CR, Byrd JP, Kumar S, Obukhov AG, Sturek M.** 2010. Exercise training decreases store-operated Ca^{2+} entry associated with metabolic syndrome and coronary atherosclerosis. Cardiovasc Res **85:**631–640.
20. **Flum DR, Devlin A, Wright AS, Figueredo E, Alyea E, Hanley PW, Lucas MK, Cummings DE.** 2007. Development of a porcine Roux-en-Y gastric bypass survival model for the study of postsurgical physiology. Obes Surg **17:**1332–1339.
21. **Friedman JM.** 2002. The function of leptin in nutrition, weight, and physiology. Nutr Rev **60:**S1–S14.
22. **Friedewald WT, Levy RI, Fredrickson DS.** 1972. Estimation of the concentration of low-density lipoprotein cholesterol in plasma, without use of the preparative ultracentrifuge. Clin Chem **18:**499–502.
23. **Gal D, Isner JM.** 1992. Atherosclerotic Yucatan microswine as a model for novel cardiovascular interventions and imaging, p 118–140. In: Swindle MM, Moody DC, Phillips LD, editors. Swine as models in biomedical research. Ames (IA): Iowa State University Press.
24. **Gerrity RG, Natarajan R, Nadler JL, Kimsey T.** 2001. Diabetes-induced accelerated atherosclerosis in swine. Diabetes **50:**1654–1665.
25. **Graier WF, Simecek S, Sturek M.** 1995. Cytochrome P450 monooxygenase-regulated signalling of Ca^{2+} entry in human and bovine endothelial cells. J Physiol **482:**259–274.
26. **Greif M, Becker A, von Ziegler F, Lebherz C, Lehrke M, Broedl UC, Tittus J, Parhofer K, Becker C, Reiser M, Knez A, Leber AW.** 2009. Pericardial adipose tissue determined by dual-source CT is a risk factor for coronary atherosclerosis. Arterioscler Thromb Vasc Biol **29:**781–786.
27. **Grundy SM.** 2007. Metabolic syndrome: a multiplex cardiovascular risk factor. J Clin Endocrinol Metab **92:**399–404.
28. **Grundy SM, Brewer HB, Cleeman JI, Smith SC Jr, Lenfant C.** 2004. Definition of the metabolic syndrome. Circulation **109:**433–438.
29. **Hainsworth DP, Katz ML, Sanders DA, Sanders DN, Wright EJ, Sturek M.** 2002. Retinal capillary basement membrane thickening in a porcine model of diabetes mellitus. Comp Med **52:**523–529.
30. **Hall JE.** 2003. The kidney, hypertension, and obesity. Hypertension **41:**625–633.

31. **Heaps CL, Sturek M, Price EM, Laughlin MH, Parker JL.** 2001. Sarcoplasmic reticulum Ca^{2+}-ATPase uptake is impaired in coronary smooth muscle distal to chronic occlusion. Am J Physiol Heart Circ Physiol **281:**H223–H231.
32. **Hill BJF, Dixon JL, Sturek M.** 2001. Effect of atorvastatin on intracellular calcium uptake in coronary smooth muscle cells from diabetic pigs fed an atherogenic diet. Atherosclerosis **159:**117–124.
33. **Hill BJF, Katwa LC, Wamhoff BR, Sturek M.** 2000. Enhanced endothelin$_A$ receptor-mediated calcium mobilization and contraction in organ cultured porcine coronary arteries. J Pharmacol Exp Ther **295:**484–491.
34. **Hill BJF, Price EM, Dixon JL, Sturek M.** 2003. Increased calcium buffering in coronary smooth muscle cells from diabetic dyslipidemic pigs. Atherosclerosis **167:**15–23.
35. **Hill BJF, Wamhoff BR, Sturek M.** 2001. Functional nucleotide receptor expression and sarcoplasmic reticulum morphology in dedifferentiated porcine coronary smooth muscle cells. J Vasc Res **38:**432–443.
36. **Hsueh W, Abel ED, Breslow JL, Maeda N, Davis RC, Fisher EA, Dansky H, McClain DA, McIndoe R, Wassef MK, Rabadan-Diehl C, Goldberg IJ.** 2007. Recipes for creating animal models of diabetic cardiovascular disease. Circ Res **100:**1415–1427.
37. **Institute for Laboratory Animal Research**. 1996. Guide for the care and use of laboratory animals. Washington (DC): National Academies Press.
38. **Johnson GJ, Griggs TR, Badimon L.** 1999. The utility of animal models in the preclinical study of interventions to prevent human coronary artery restenosis: analysis and recommendations. Thromb Haemost **81:**835–843.
39. **Korte FS, Mokelke EA, Sturek M, McDonald KS.** 2005. Exercise improves impaired ventricular function and alterations of cardiac myofibrillar proteins in diabetic dyslipidemic pigs. J Appl Physiol **98:**461–467.
40. **Kreutz RP, Alloosh M, Neeb ZP, Kreutz Y, Flockhart DA, Sturek M.** 2009. Metabolic syndrome in Ossabaw miniature swine is associated with increased sensitivity of platelet aggregation to adenosine diphosphate. [(abstract)] Arterioscler Thromb Vasc Biol. **29:**e122.
41. **Kumar B, Dreja K, Shah SS, Cheong A, Xu SZ, Sukumar P, Naylor J, Forte A, Cipollaro M, McHugh D, Kingston PA, Heagerty AM, Munsch CM, Bergdahl A, Hultgardh-Nilsson A, Gomez MF, Porter KE, Hellstrand P, Beech DJ.** 2006. Upregulated TRPC1 channel in vascular injury in vivo and its role in human neointimal hyperplasia. Circ Res **98:**557–563.
42. **Langohr IM, HogenEsch H, Stevenson GW, Sturek M.** 2008. Vascular-associated lymphoid tissue in swine (*Sus scrofa*). Comp Med **58:**168–173.
43. **Larsen MO, Juhl CB, Porksen N, Gotfredsen CF, Carr RD, Ribel U, Wilken M, Rolin B.** 2005. β-Cell function and islet morphology in normal, obese, and obese β-cell mass-reduced Gottingen minipigs. Am J Physiol Endocrinol Metab **288:**E412–E421.
44. **Larsen MO, Rolin B.** 2004. Use of the Gottingen minipig as a model of diabetes with special focus on type 1 diabetes research. ILAR J **45:**303–313.
45. **Larsen MO, Rolin B, Raun K, Bjerre Knudsen L, Gotfredsen CF, Bock T.** 2007. Evaluation of β-cell mass and function in the Gottingen minipig. Diabetes Obes Metab **9 Suppl 2:**170–179.
46. **Larsen MO, Rolin B, Sturis J, Wilken M, Carr RD, Porksen N, Gotfredsen CF.** 2006. Measurements of insulin responses as predictive markers of pancreatic β-cell mass in normal and β-cell-reduced lean and obese Gottingen minipigs in vivo. Am J Physiol Endocrinol Metab **290:**E670–E677.
47. **Larsen MO, Rolin B, Wilken M, Carr RD, Gotfredsen CF.** 2003. Measurements of insulin secretory capacity and glucose tolerance to predict pancreatic β-cell mass in vivo in the nicotinamide–streptozotocin Gottingen minipig, a model of moderate insulin deficiency and diabetes. Diabetes **52:**118–123.
48. **Larsen MO, Rolin B, Wilken M, Carr RD, Svendsen O.** 2002. High-fat high-energy feeding impairs fasting glucose and increases fasting insulin levels in the Gottingen minipig: results from a pilot study. Ann N Y Acad Sci **967:**414–423.
49. **Larsen MO, Wilken M, Gotfredsen CF, Carr RD, Svendsen O, Rolin B.** 2002. Mild streptozotocin diabetes in the Göttingen minipig: a novel model of moderate insulin deficiency and diabetes. Am J Physiol Endocrinol Metab **282:**E1342–E1351.
50. **Le TT, Langohr IM, Locker MJ, Sturek M, Cheng JX.** 2007. Label-free molecular imaging of atherosclerotic lesions using multimodal nonlinear optical microscopy. J Biomed Opt **12:**054007.
51. **Lee DL, Wamhoff BR, Katwa LC, Reddy HK, Voelker DJ, Dixon JL, Sturek M.** 2003. Increased endothelin-induced Ca^{2+} signaling, tyrosine phosphorylation, and coronary artery disease in diabetic dyslipidemic swine are prevented by atorvastatin. J Pharmacol Exp Ther **306:**132–140.
52. **Lee L, Alloosh M, Saxena R, Van Alstine W, Watkins BA, Klaunig JE, Sturek M, Chalasani N.** 2009. Nutritional model of steatohepatitis and metabolic syndrome in the Ossabaw miniature swine. Hepatology **50:**56–67.
53. **Levy J, Gavin JR, Sowers JR.** 1994. Diabetes mellitus: A disease of abnormal cellular calcium metabolism? Am J Med **96:**260–273.
54. **Lloyd PG, Fang M, Brisbin IL Jr, Andersson L, Sturek M.** 2006. AMP kinase gene mutation is consistent with a thrifty phenotype (metabolic syndrome) in a population of feral swine. FASEB J **20:**A299.
55. **Lloyd PG, Sheehy AF, Edwards JM, Mokelke EA, Sturek M.** 2008. Leukemia inhibitory factor is upregulated in coronary arteries of Ossabaw miniature swine after stent placement. Coron Artery Dis **19:**217–226.
56. **Lovejoy JC, Windhauser MM, Rood JC, de la Bretonne JA.** 1998. Effect of a controlled high-fat versus low-fat diet on insulin sensitivity and leptin levels in African-American and Caucasian women. Metabolism **47:**1520–1524.
57. **Lowe HC, Schwartz RS, Mac Neill BD, Jang IK, Hayase M, Rogers C, Oesterle SN.** 2003. The porcine coronary model of in-stent restenosis: current status in the era of drug-eluting stents. Catheter Cardiovasc Interv **60:**515–523.
58. **Maclean N, Ogilvie RF.** 1955. Quantitative estimation of the pancreatic islet tissue in diabetic subjects. Diabetes **4:**367–376.
59. **Martin RJ, Gobble JL, Hartsock TH, Graves HB, Ziegler JH.** 1973. Characterization of an obese syndrome in the pig. Proc Soc Exp Biol Med **143:**198–203.
60. **Masuzaki H, Paterson J, Shinyama H, Morton NM, Mullins JJ, Seckl JR, Flier JS.** 2001. A transgenic model of visceral obesity and the metabolic syndrome. Science **294:**2166–2170.
61. **Mokelke EA, Dietz NJ, Eckman DM, Nelson MT, Sturek M.** 2005. Diabetic dyslipidemia and exercise affect coronary tone and differential regulation of conduit and microvessel K^+ current. Am J Physiol Heart Circ Physiol **288:**H1233–H1241.
62. **Mokelke EA, Hu Q, Song M, Toro L, Reddy HK, Sturek M.** 2003. Altered functional coupling of coronary K^+ channels in diabetic dyslipidemic pigs is prevented by exercise. J Appl Physiol **95:**1179–1193.
63. **Moreno PR, Fallon JT, Murcia AM, Leon MN, Simosa H, Fuster V, Palacios IF.** 1999. Tissue characteristics of restenosis after percutaneous transluminal coronary angioplasty in diabetic patients. J Am Coll Cardiol **34:**1045–1049.
64. **Morgan KP, Kapur A, Beatt KJ.** 2004. Anatomy of coronary disease in diabetic patients: an explanation for poorer outcomes after percutaneous coronary intervention and potential target for intervention. Heart **90:**732–738.
65. **Natali A, Vichi S, Landi P, Severi S, L'Abbate A, Ferrannini E.** 2000. Coronary atherosclerosis in type II diabetes: angiographic findings and clinical outcome. Diabetologia **43:**632–641.
66. **Neeb ZP, Edwards JM, Bratz IN, Alloosh M, Schultz C, Thompson K, Cunha T, and Sturek M**. 2008. Occlusive, diffuse coronary artery disease in Ossabaw miniature swine with metabolic syndrome. FASEB J **22:**1152.10.
67. **Nicholls SJ, Tuzcu EM, Kalidindi S, Wolski K, Moon KW, Sipahi I, Schoenhagen P, Nissen SE.** 2008. Effect of diabetes on progression of

coronary atherosclerosis and arterial remodeling: a pooled analysis of 5 intravascular ultrasound trials. J Am Coll Cardiol **52:**255–262.
68. **Otis CR, Wamhoff BR, Sturek M.** 2003. Hyperglycemia-induced insulin resistance in diabetic dyslipidemic Yucatan swine. Comp Med **53:**53–64.
69. **Owens GK, Kumar MS, Wamhoff BR.** 2004. Molecular regulation of vascular smooth muscle cell differentiation in development and disease. Physiol Rev **84:**767–801.
70. **Panepinto LM, Phillips RW, Westmoreland NW, Cleek JL.** 1982. Influence of genetics and diet on the development of diabetes in Yucatan miniature swine. J Nutr **112:**2307–2313.
71. **Peterson RG.** 2001. The Zucker diabetic fatty (ZDF) rat, p 109–128. In: Sima AAF, Shafrir E, editors. Animal models of diabetes: a primer. Amsterdam (Netherlands): Harwood Academic Publishers.
72. **Phillips RW, Panepinto LM, Spangler R, Westmoreland N.** 1982. Yucatan miniature swine as a model for the study of human diabetes mellitus. Diabetes **31:**30–36.
73. **Phillips RW, Westmoreland N, Panepinto L, Case GL.** 1982. Dietary effects on metabolism of Yucatan miniature swine selected for low and high glucose utilization. J Nutr **112:**104–111.
74. **Piatti P, Di Mario C, Monti LD, Fragasso G, Sgura F, Caumo A, Setola E, Lucotti P, Galluccio E, Ronchi C, Origgi A, Zavaroni I, Margonato A, Colombo A.** 2003. Association of insulin resistance, hyperleptinemia, and impaired nitric oxide release with in-stent restenosis in patients undergoing coronary stenting. Circulation **108:**2074–2081.
75. **Pons D, Monraats PS, Zwinderman AH, de Maat MPM, Doevendans PAFM, de Winter RJ, Tio RA, Waltenberger J, Jukema JW.** 2009. Metabolic background determines the importance of *NOS3* polymorphisms in restenosis after percutaneous coronary intervention: a study in patients with and without the metabolic syndrome. Dis Markers **26:**75–83.
76. **Rana JS, Monraats PS, Zwinderman AH, de Maat MPM, Kastelein JJP, Doevendans PAF, de Winter RJ, Tio RA, Frants RR, van der Laarse A, van der Wall EE, Jukema JW.** 2005. Metabolic syndrome and risk of restenosis in patients undergoing percutaneous coronary intervention. Diabetes Care **28:**873–877.
77. **Rector RS, Thomas TR, Liu Y, Henderson KK, Holiman DA, Sun GY, Sturek M.** 2004. Effect of exercise on postprandial lipemia following a higher calorie meal in Yucatan miniature swine. Metabolism **53:**1021–1026.
78. **Sacks DB, Bruns DE, Goldstein DE, Maclaren NK, McDonald JM, Parrott M.** 2002. Guidelines and recommendations for laboratory analysis in the diagnosis and management of diabetes mellitus. Clin Chem **48:**436–472.
79. **Schwartz RS, Edelman ER.** 2002. Drug-eluting stents in preclinical studies. Recommended evaluation from a consensus group. Circulation **106:**1867–1873.
80. **Sheehy A, Mokelke EA, Lloyd PG, Sturek J, Sturek M.** 2006. Reduced expression of leukemia inhibitory factor correlates with coronary atherosclerosis in the metabolic syndrome. FASEB J **20:**A698.
81. **Stehno-Bittel L, Laughlin MH, Sturek M.** 1990. Exercise training alters Ca^{2+} release from coronary smooth muscle sarcoplasmic reticulum. Am J Physiol **259:**H643–H647.
82. **Stehno-Bittel L, Laughlin MH, Sturek M.** 1991. Exercise training depletes sarcoplasmic reticulum calcium in coronary smooth muscle. J Appl Physiol **71:**1764–1773.
83. **Sturek M, Alloosh M, Wenzel J, Byrd JP, Edwards JM, Lloyd PG, Tune JD, March KL, Miller MA, Mokelke EA, Brisbin IL Jr.** 2007. Ossabaw Island miniature swine: cardiometabolic syndrome assessment, p 397–402. In: Swindle MM, editor. Swine in the laboratory: surgery, anesthesia, imaging, and experimental techniques. Boca Raton (FL): CRC Press.
84. **Takagi T, Yoshida K, Akasaka T, Kaji S, Kawamoto T, Honda Y, Yamamuro A, Hozumi T, Morioka S.** 2000. Hyperinsulinemia during oral glucose tolerance test is associated with increased neointimal tissue proliferation after coronary stent implantation in nondiabetic patients: a serial intravascular ultrasound study. J Am Coll Cardiol **36:**731–738.
85. **Tommasino A, Burzotta F, Trani C, Giammarinaro M, Schiavoni G.** 2008. Impact of metabolic syndrome on angiographic and clinical outcome after stenting. Am J Cardiol **101:**1679.
86. **Touchard AG, Schwartz RS.** 2006. Preclinical restenosis models: challenges and successes. Toxicol Pathol **34:**11–18.
87. **Turk JR, Carroll JA, Laughlin MH, Thomas TR, Casati J, Bowles DK, Sturek M.** 2003. C-reactive protein correlates with macrophage accumulation in coronary arteries of hypercholesterolemic pigs. J Appl Physiol **95:**1301–1304.
88. **Wallace TM, Levy JC, Matthews DR.** 2004. Use and abuse of HOMA modeling. Diabetes Care **27:**1487–1495.
89. **Wamhoff BR, Bowles DK, Dietz NJ, Hu Q, Sturek M.** 2002. Exercise training attenuates coronary smooth muscle phenotypic modulation and nuclear Ca^{2+} signaling. Am J Physiol Heart Circ Physiol **283:**H2397–H2410.
90. **Wamhoff BR, Bowles DK, McDonald OG, Sinha S, Somlyo AP, Owens GK.** 2004. L-type voltage-gated Ca^{2+} channels modulate expression of smooth muscle differentiation marker genes via a Rho kinase–myocardin–SRF-dependent mechanism. Circ Res **95:**406–414.
91. **Wamhoff BR, Dixon JL, Sturek M.** 2002. Atorvastatin treatment prevents alterations in coronary smooth muscle nuclear Ca^{2+} signaling associated with diabetic dyslipidemia. J Vasc Res **39:**208–220.
92. **Wang HW, Langohr IM, Sturek M, Cheng JX.** 2009. Imaging and quantitative analysis of atherosclerotic lesions by CARS-based multimodal nonlinear optical microscopy. Arterioscler Thromb Vasc Biol **29:**1342–1348.
93. **Warnick GR, Benderson J, Albers JJ.** 1982. Dextran sulfate–Mg^{2+} precipitation procedure for quantitation of HDL cholesterol. Clin Chem **28:**1379–1388.
94. **Wilson PW, D'Agostino RB, Parise H, Sullivan L, Meigs JB.** 2005. Metabolic syndrome as a precursor of cardiovascular disease and type 2 diabetes mellitus. Circulation **112:**3066–3072.
95. **Witczak CA, Mokelke EA, Boullion RD, Wenzel J, Keisler DH, Sturek M.** 2005. Noninvasive measures of body fat percentage in male Yucatan swine. Comp Med **55:**445–451.
96. **Witczak CA, Sturek M.** 2004. Exercise prevents diabetes-induced impairment in superficial buffer barrier in porcine coronary smooth muscle. J Appl Physiol **96:**1069–1079.
97. **Witczak CA, Sturek M.** 2005. Training-induced sarcoplasmic reticulum Ca^{2+} unloading occurs without Ca^{2+} influx. Med Sci Sports Exerc **37:**1119–1125.
98. **Witczak CA, Wamhoff BR, Sturek M.** 2006. Exercise training prevents Ca^{2+} dysregulation in coronary smooth muscle from diabetic dyslipidemic Yucatan swine. J Appl Physiol **101:**752–762.